EXPERIMENTAL EVALUATION OF THE STATIC AND DYNAMIC CHARACTERISTICS OF AN OFFSHORE CRANE MODEL

(Date received: 24.10.2008)

T. L. Chan[1], J. I. Inayat-Hussain[2], K. S. Teoh[1] and Y. T. Liew[3]
[1]*School of Engineering, Monash University, Jalan Lagoon Selatan, 46150 Bandar Sunway, Selangor Darul Ehsan*
[2]*College of Engineering, Universiti Tenaga Nasional, Km 7 Jalan Kajang-Puchong, 43009 Kajang, Selangor Darul Ehsan*
[3]*Favelle Favco Berhad, Lot 586, 2nd Mile, Jalan Batu Tiga Lama, 41300, Klang, Selangor Darul Ehsan*
E-mail: [1]tlcha6@student.monash.edu

ABSTRACT

The knowledge of the static and dynamic characteristics of cranes is of utmost importance in their design and construction in order to optimise the construction material costs as well as to optimize their response to static and dynamic loadings during operation. Although numerical simulation of the crane response subjected to various loading conditions are routinely undertaken in the design stage, experimental verification of these numerical results are rarely performed due to the high cost involved. Experimental verification of the static and dynamic characteristics of these cranes can however be performed at a significantly lower cost on their scaled-down models. The results from the scaled-down models provide useful insights into the static and dynamic performance of these cranes. In the work presented herein, a scaled-down model of a boom angle luffing crane prototype, typically employed in offshore engineering applications, was developed using dimensionless p parameters. The model, which has geometric and dynamic similarities with the prototype, was numerically and experimentally examined for its static and dynamic characteristics. The numerical analysis of the model was undertaken using a commercially available finite-element computer program, ANSYS. This program was utilized to compute the stiffness and stresses in the model subjected to static loads, as well as the natural frequencies and mode shapes, which represent the dynamic characteristics of the model. An experimental rig was fabricated based on the scaled-down model, and measurements were performed to verify the computational results obtained from the finite-element analysis. The static strains measured at various positions on the boom were found to be within 14% of those obtained numerically. The natural frequencies and mode shapes of the model crane were obtained using modal testing technique and were found to be in good agreement to those obtained numerically, with discrepancies within 3% for the first three modes.

Keywords: *Dynamic Characteristics, Finite-element Analysis, Modal Testing, Offshore Crane and Static*

1.0 INTRODUCTION

In the design and construction of cranes the knowledge of their static and dynamic characteristics are of significant importance to optimize the construction material costs, their response to static loading due to suspension of the payload at different boom angles, and their response to dynamic loading due to acceleration of the payload during lifting and lowering operations. Offshore cranes in particular, are subjected to dynamic loading arising from ocean waves that cause the payload to rise and fall following the movement of these waves. The movement of these waves creates a relative velocity between the boom tip and the load, which in turn causes the boom to vibrate. The design of cranes requires the information on their dynamic properties, namely the natural frequencies and mode shapes. This information is essential for the development of suitable loading charts for the cranes [1] as well as for the incorporation of vibration absorbers in the design of these cranes [2].

Although numerical simulation of the crane response subjected to various static and dynamic loading conditions are routinely undertaken in the design stage, experimental verification of these numerical results are rarely performed due to the high cost involved. Experimental verification of the static and dynamic characteristics of these cranes can however be performed at a significantly lower cost on their scaled-down models. The results from the scaled-down models provide useful insights into the static and dynamic performance of these cranes.

Andreu *et al*. [3] employed the finite-element method to create deformable catenary elements that were used to simulate cable net systems by combining multiple elements. In order to create a more realistic model for a mobile crane, Sun *et al.* [4] coupled the drive system of the hoist along with the boom, which was modeled using nonlinear elements for the ropes and Timoshenko beam elements for the truss lattice structure. The cross section of the beam element for the boom was selected so that its stiffness was equivalent to the section of the truss lattice structure. Ju and Choo [5, 6] modeled a boom angle luffing crane using parameterised super elements to represent the 1 cabling system where the cable was modeled as a single element, and the cable passage over the pulleys was represented as a new degree of freedom. The boom and mast were represented as planar frame elements as the emphasis of the work was on the performance of the cable system. Wu *et al.* [7] and Wu [8,9] used finite-element method to model a gantry crane subjected to time varying loads. Shape functions were used to determine the location and magnitude of the force acting on the beam.

While computer simulations provide a convenient method of predicting the behavior of complex systems such as the dynamic characteristic of a crane, they are only as good as the assumptions that are included in the construction of the model. This largely lies in the experience of the modeler and the capabilities of the computer algorithms. Experimental verification can highlight neglected characteristics or underestimated assumptions, which can lead to a better model. Once the model has been successfully verified, it can be used for more complex simulations. For dynamic analysis, verification is carried out using modal identification techniques, which involve extraction of mode shapes and natural frequencies as they are exclusive to individual structures. Wu [8,9] built a 1/10 scaled experimental gantry crane model to verify a similar scaled-down model created using the finite-element method. Various issues that affected the compatibility between the experimental model and the finite-element model were identified. Jerman *et al.* [10] and Jerman [11] used a physical model to verify the characteristics of a slewing crane's mathematical model. The input to both models was via a velocity profile graph. Air friction and slewing ring resistance were also accounted for in these models. Al-Sweiti and Söffker [12] modeled the lower half of a ship mounted boom angle luffing crane using beam element to account for the flexural elasticity of the boom. The upper part of the boom where the rigging of the hoist rope is located was considered as rigid in their model. Their experimental rig was capable of simulating roll conditions through the use of a hydraulic cylinder to swing the entire crane structure. Henry *et al.* [13] used a test rig that was capable of simulating pitch, heave and roll of a ship mounted crane using a Carpal wrist 2 mechanism actuated using servo motors. The test rig was used to investigate the pendulation of the payload in a ship mounted boom angle luffing crane.

In the work presented herein, a numerical model and an experimental test rig that are based on a scaled-down model of a boom angle luffing crane prototype were analysed for compatibility. The scaled-down model was designed to include geometric and dynamic similarities with the prototype. The compatibility analysis was carried out by comparing the static and dynamic behaviour of both models. The numerical analysis of the model was undertaken using the finite-element computer program, ANSYS. This program was utilised to compute the stiffness and stresses in the model subjected to static loads, as well as the natural frequencies and mode shapes, which represent the dynamic characteristics of the model. The experimental rig of the model crane was analysed for its static and dynamic behaviour through static strain load test and frequency response test using an instrumented hammer to obtain its natural frequencies and mode shapes for verification of the computational results obtained from the finite-element analysis.

2.0 DESIGN OF THE SCALED-DOWN MODEL

The main components of the boom angle luffing crane, also known as the critical components [14], are the boom, luff, hoist ropes and the payload. These components determine the stiffness of the crane and were included in the scaled-down model developed in this work, Figure 1. The boom consists of a square hollow section. The vertical stiffness of the beam was designed to be dynamically similar to that of the prototype.

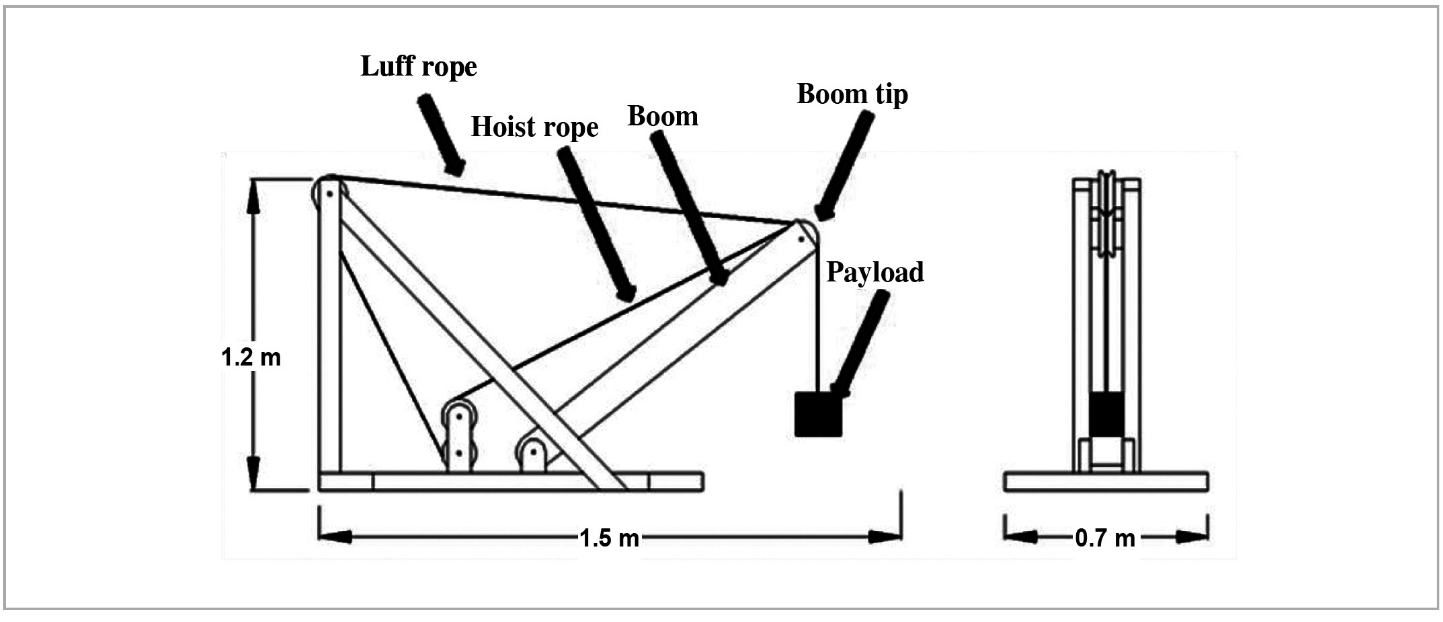

Figure 1: Schematic of the scaled-down model of the offshore boom angle luffing crane

The dimensions of the boom and wire rope stiffness were determined using the dimensionless groups. Three parameters were used to represent the geometry and dynamics of the crane. For geometric similarity, the relative distances between the boom pivot, mast head sheave, boom tip and the hoist and luff rope winch drum were arranged based on the relative distances of the prototype so that the lever arm lengths for the luff ropes and the vertical and inclined hoist ropes of the test rig were in proportion to the lever arm lengths of the full scaled prototype. The dimensionless parameters, which scaled the critical components of the model geometrically, were proposed by Jones [15] and are reproduced in Equations (1) and (2).

The dynamic characteristics of the model to the prototype were scaled using the equation proposed by Wu *et al*. [7] and reproduced in Equation (3). n w represents the natural frequency of the crane system and the variable t represents the time taken for the amplitude of the vibration to reach half of the maximum amplitude. These equations were derived using the Buckingham Pi theorem. To derive Equations (1) and (2), it was assumed that the static behaviour of the crane is a function of the boom length, boom cross sectional area, boom tip displacement, mass of the payload, gravity and force while in to derive Equation (3), it was assumed that the dynamic behaviour of the crane is a function of the displacement, damping ratio, natural frequency, mass, time and force. From the various combinations of dimensionless groups, these three groups were selected based on the availability of information on the behaviour of the crane.

$$\pi_1 = \frac{\textit{Boom tip displacement}}{\textit{Boom length}} \tag{1}$$

$$\pi_2 = \frac{\textit{Boom tip displacement}}{\sqrt{\textit{Boom cross section area}}} \tag{2}$$

$$\pi_3 = \omega_n t \tag{3}$$

The stiffness of the boom angle luffing crane prototype was computed by Lee and Gan [16] by loading their model with a 1 ton force at the maximum boom angle of 85° and calculating the resulting displacement. In order to determine the stiffness of the scaled-down model, iterations were carried out for various boom cross sectional areas and the payload sizes until matching dimensionless values were obtained. Table 1 shows the parameters used to calculate the values of the non dimensional groups. The size of the scaled test load that results in the values for the first and second non-dimensional group was found to be 2 kg and the dimensions of the boom cross section were 12.7 mm by 12.7 mm, with thickness of 0.4 mm. The elasticity of the steel wire rope, consisting of six strands of seven wires, used in the scaled-down model was estimated to be 80 GPa [17]. The resulting values of the non dimensional groups with the said boom dimensions are shown in Table 2. This set of values are the closest obtained from iterative analysis with various payload, rope and boom sizes, which indicates that this is the best scaled model to represent the full scaled prototype.

Table 1: Values of the parameters in the non – dimensional groups

	Model	Prototype
Boom tip displacement (m)	2.81×10^{-4}	0.006
Boom length (m)	1.5	36.6
Boom effective cross section area (m^2)	3.81×10^{-5}	0.01056
Natural frequency (rad/s)	210.5	6.28
Time (s)	0.1	2.5

Table 2: Comparison of the values of the non – dimensional groups between the scaled-downdown model and prototype

	Model	Prototype
$\pi 1$	1.9×10^{-4}	1.6×10^{-4}
$\pi 2$	0.046	0.058
$\pi 3$	21.05	15.7

3.0 NUMERICAL RESULTS

The displacement of the boom tip of the scaled-down model due to static loading was computed using ANSYS for two extreme conditions, *i.e.*, largest boom angle of 85° and smallest boom angle of 20°. These angles are the limits of the luffing angle and are often used for operational tests by crane manufacturers. The loading applied at the boom tip was 19.62 N. The material properties and elements used are shown in Table 3. The boom was modeled using beam elements while the ropes were modeled using single link element each since no lateral vibration was expected along the ropes. Vertical and horizontal displacement constraints were applied at the free nodes of the luff and hoists ropes and the boom while a downward vertical force of 2 kg was applied at the boom tip to simulate the payload. The finite element model is shown in Figure 2.

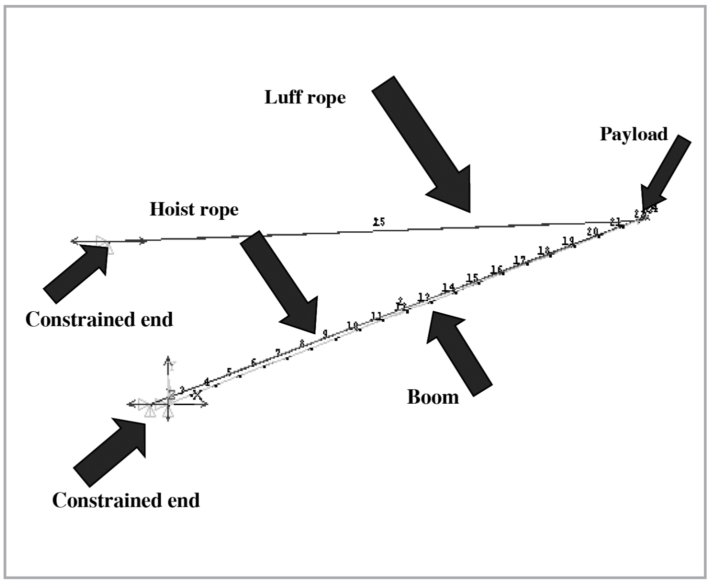

Figure 2: The finite element model at boom angle of 20°

Table 3: Material properties and element used for the crane components

Component	Material properties	Element
Boom	Steel Modulus of Elasticity: 200 GPa Density: 7870 kg/m^3 Poisson Ratio: 0.29	BEAM 3 Euler Bernoulli 3D Beam
Ropes of luff and hoist line	Steel rope Modulus of Elasticity : 80 GPa Density 7870 kg/m^3	LINK 8 uniaxial structural link
Payload	Mass : 2 kg	MASS 21 Structural point mass
Connection between components	None	MPC 184 rigid beam element

The static load results for these two conditions are shown in Table 4 and graphically represented in Figure 3. The darker and lighter shades represent compressive and tensile loading respectively.

Table 4: Static displacement results for the two extreme conditions of the boom angle

	Boom Angle 85°	Boom Angle 20°
Boom tip displacement (m)	1.234×10^{-6}	0.034
Compressive force on boom (N)	28.2	61.7
Tensile force in luff rope (N)	5.5	51.91

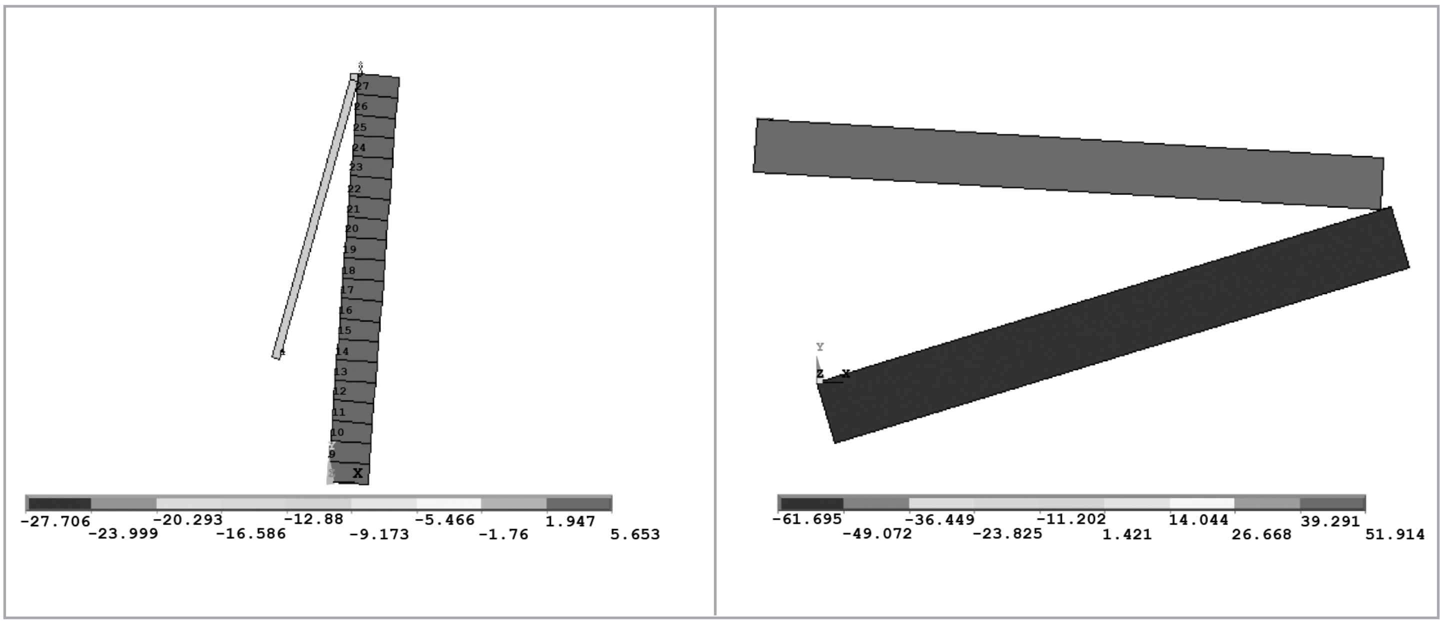

Figure 3: Tensile and compressive force contours of the finite element model for boom angle: (a) 85°, (b) 20°

From the static simulation with the two extreme boom angles, it was found that the boom experiences compression while the luff and hoist ropes undergo tension. The tensile and compressive forces are larger with the boom angle of 20^o. This is due to the larger pulling of the luff rope, which produced a larger compression in the boom. This confirms the analysis by Charrett and Hyden[14] on static loading of boom angle luffing cranes where the lowest boom angle was identified as the maximum loading angle.

The natural frequencies and mode shapes of the scaled-down model were determined using the Block Lanczos mode extraction method [18] that is available in the modal analysis module of the ANSYS finite element analysis software. The analysis was repeated with increasing number of beam elements to obtain a converged solution on the modal parameters. To avoid discretization errors in higher mode shapes, 20 beam elements were used to model the boom and to obtain a converged solution. The elements used for this model are shown in Table 3. The same displacement constraints were applied for this model with the exception of the loading that was omitted and replaced with the mass element. The boom was aligned at 20° for this analysis, which is the same angle used for the experimental verification. The simulation results are shown in Table 9.

4.0 EXPERIMENTAL VERIFICATION OF THE FINITE-ELEMENT MODEL

An experimental rig representing the scaled-down model, as shown in Figure 4, was built and instrumented with strain gauges as shown in Figure 5. The strain gauges were attached to the experimental rig at five different positions, *i.e.*, the base, lower-half, mid-span and upper-half of the boom, and the boom tip. In the static displacement test, a range of test load similar to the loads used in the static simulation using the finite element model was applied at the boom tip. The static strains were measured at all the points where the strain gauges were attached and compared to the simulated results to to check for compatibility between the finite element model and experimental test rig. The boom angle was fixed at 20^o during the experimental work. Experimental values of the strain are compared to those obtained from the finite-element analysis as shown in Tables 5 to 8. Results indicate percentage errors of less than 13% between the measured strains with those computed using ANSYS.

Figure 4: Experimental rig representing scaled-down model of an offshore crane

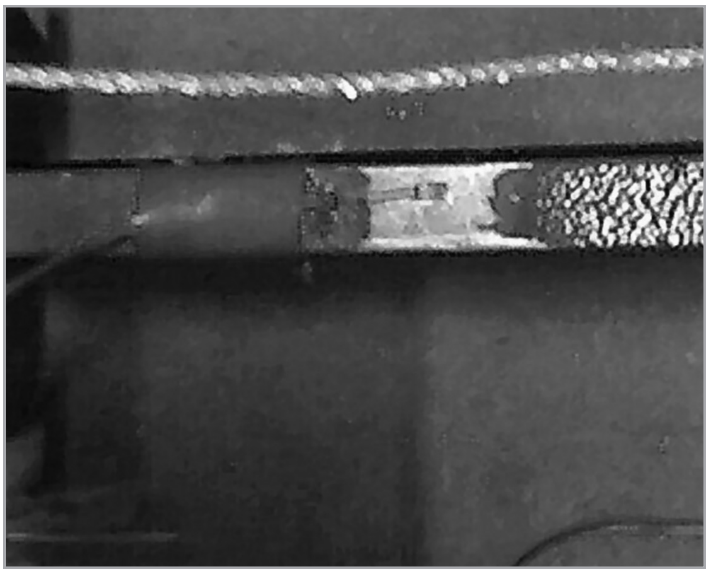

Figure 5: A strain gauge attached to the boom

Table 5: Comparison between the measured and simulated strain with a 10 N payload

	Measured	Simulated	% Error
Base	-4.85E-07	-5.24E-007	7.43
Lower half	-2.75E-06	-3.14E-006	12.52
Mid span	-5.47E-06	-5.76E-006	5.08
Upper half	-8.03E-06	-8.38E-006	4.21
Tip	-9.89E-06	-1.05E-005	5.61

Table 6: Comparison between the measured and simulated strain with a 20 N payload

	Measured	Simulated	% Error
Base	-8.50E-07	-8.98E-007	5.35
Lower half	-4.96E-06	-5.39E-006	7.95
Mid span	-9.59E-06	-9.88E-006	2.92
Upper half	-1.32E-05	-1.44E-005	8.14
Tip	-1.61E-05	-1.80E-005	10.36

Table 7: Comparison between the measured and simulated strain with a 30 N payload

	Measured	Simulated	% Error
Base	-1.40E-06	-1.27E-006	10.04
Lower half	-7.20E-06	-7.63E-006	5.69
Mid span	-1.37E-05	-1.40E-005	2.11
Upper half	-1.92E-05	-2.04E-005	5.68
Tip	-2.35E-05	-2.54E-005	7.65

Table 8: Comparison between the measured and simulated strain with a 40 N payload

	Measured	Simulated	% Error
Base	-1.81E-06	-1.65E-006	9.93
Lower half	-9.45E-06	-9.88E-006	4.34
Mid span	-1.78E-05	-1.81E-005	1.72
Upper half	-2.51E-05	-2.63E-005	4.72
Tip	-3.08E-05	-3.29E-005	6.47

In the verification of the dynamic properties of the scaled-down model computed using finiteelement analysis, modal testing was undertaken on the experimental rig to determine its natural frequencies and mode shapes. The modal extraction methods are well established and their details may be found in Ewins [19]. Twenty-one points corresponding to the nodes in the finite-element model of this rig were identified along the boom. An instrumented hammer, as shown in Figure 6, was used to apply impulsive force on these points and the response of the boom was measured using an accelerometer, as shown in Figure 7. The accelerometer was attached to the tip of the boom since large oscillations were expected there. The output signal from the hammer and accelerometer was fed into a dual channel spectrum analyser to obtain the natural frequencies and mode shapes of the test rig.

The natural frequencies measured for the first three modes are compared with those obtained using finite-element analysis in Table 9. The agreement between the measured and the computed natural frequencies was good with percentage errors less than 3%. The results further indicate that the finite-element computation overestimates the natural frequencies. This is because the finite element model is defined by a finite number of elements and thus it is stiffer than the experimental model. This is evident by the larger natural frequencies obtained from the simulated results. In addition to that, experimental results were affected by friction in the moving components and less than ideal boundary conditions. However the experimental mode shapes also compared relatively well with those computed as shown in Figure 8. The experimental mode shape results could have been improved if more points on the boom were used in the modal test.

Figure 6: Instrumented hammer for the experimental modal analysis

Figure 7: Accelerometer attached to the boom tip to measure dynamic response

Table 9: Comparison between the computed and measured natural frequencies

Mode No.	Finite-Element Analysis (Hz)	Experimental (Hz)	% Error
1	8.5	8.3	2.4
2	16.3	15.9	2.5
3	101.8	98.7	3.0

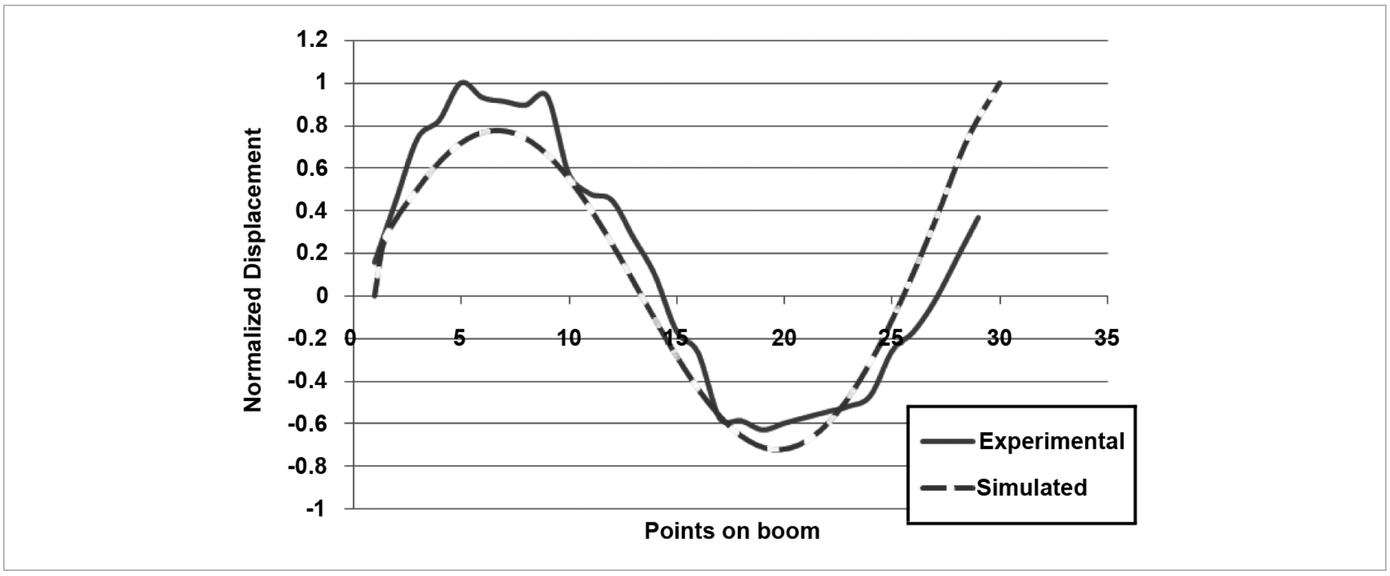

(a)

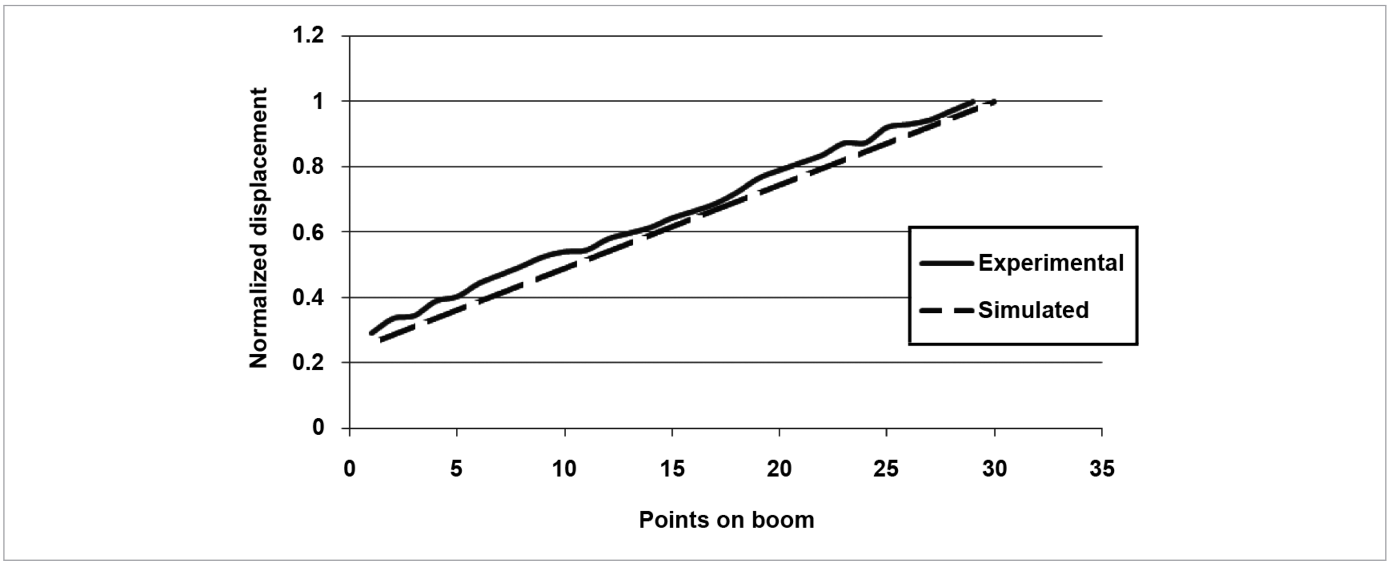

(b)

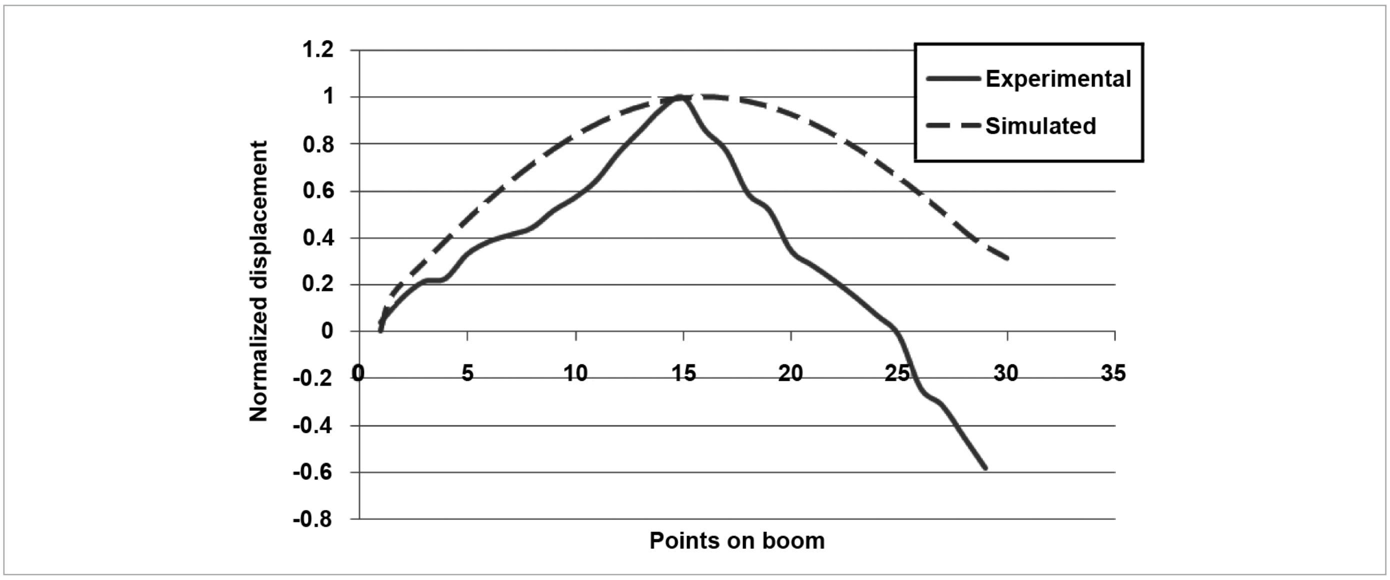

(c)

Figure 8: Comparison between the simulated and measured mode shapes: (a) first mode, (b) second mode, (c) third mode

5.0 CONCLUSION

The development of a scaled-down model of a boom angle luffing crane prototype using dimensionless π parameters is presented in this work. The model, which has geometric and dynamic similarities with the prototype, was numerically and experimentally examined for its static and dynamic characteristics. The numerical analysis of the model was undertaken using a commercially available finite-element computer program, ANSYS. This program was utilised to compute the stiffness and stresses in the model subjected to static loads, as well as the natural frequencies and mode shapes, which represent the dynamic characteristics of the model. An experimental rig of the model crane was fabricated, and measurements were performed to verify the computational results obtained from the finite-element analysis. The static strains measured at various positions on the boom were found to be within 14% of those obtained from the finiteelement analysis. The natural frequencies and mode shapes of the model crane obtained using modal testing technique was also found to be in good agreement to those obtained from the finiteelement analysis, with discrepancies within 3% for the first three modes. The numerical and experimental results from the scaled-down model may provide useful insights into the static and dynamic performance of the prototype cranes. They also serve as a less expensive alternative to evaluate the static and dynamic characteristics of prototype cranes, as full scaled testing of these prototypes are rarely undertaken due to the exorbitant cost involved. ■

REFERENCES

[1] J. Verschoof, Crane Design, Practice and Maintenance, Suffolk: Professional Engineering Publishing, 2002.

[2] W. Lacarbonara, R. R. Soper, A. H. Nayfeh and D. Mook, A Non Classical Vibration Absorber for Pendulation Reduction, Journal of Vibration and Control 7 (2001) 365-393.

[3] A. Andreu, L. Gil and P. Roca, A New Deformable Catenary Element for the Analysis of Cable Net Structures, Computers and Structures 84 (2006) 1882 – 1890.

[4] G. Sun, M. Kleeberger and J. Liu, Complete Dynamic Calculation of Lattice Mobile Crane During Hoisting Motion, Mechanism and Machine Theory 40 (2004) 447 – 466.

[5] F. Ju and Y.S. Choo, Super Element Approach to Cable Passing Through Multiple Pulleys, International Journal of Solids and Structures 42 (2004) 3533 – 3547.

[6] F. Ju, Y.S. Choo, Dynamic Analysis of Tower Cranes, Journal of Engineering Mechanics 131 (2005) 88 – 96.

[7] J. J. Wu, M.P. Cartmell and A. R. Whittaker, Prediction of the Vibration Characteristics of a Full Sized Structure from those of a Scaled Model, Computers and Structures 80 (2001) 1461 – 1472.

[8] J. J. Wu, Finite Element Modelling and Experimental Modal Testing of a Three Dimensional Framework, International Journal of Mechanical Sciences 46 (2004)1245 – 1266.

[9] J. J. Wu, Finite Element Analysis and Vibration Testing of a Three – Dimensional Crane Structure, Measurement 39 (2004) 740 – 749.

[10] B. Jerman, P. Podržaj and J. Kramar, An Investigation of Slewing – Crane Dynamics During Slewing Motion – Development and Verification of a Mathematical Model, International Journal of Mechanical Sciences 46 (2004) 729 – 750.

[11] B. Jerman, An Enhanced Mathematical Model for Investigating the Dynamic Loading of a Slewing Crane, Proceedings of the Institution of Mechanical Engineers 220 (2005) 421 – 433.

[12] Y. Al – Sweiti and D. Söffker, Planar Cargo Control of Elastic Ship Cranes with the Maryland Rigging System, Journal of Vibration and Control 13 (2007) 241.

[13] R. J. Henry, Z. N. Masoud, A. H. Nayfeh and D. T. Mook, Cargo Pendulation Reduction on Ship – Mounted Cranes Via Boom – Luff Angle Actuation, Journal of Vibration and Control 7 (2001) 1253.

[14] D. E. Charrett and A. M. Hyden, Dynamic Factors for Offshore Cranes, Proceedings of 8th Annual Offshore Technology Conference, Houston, Dallas, May 3 – 6, 1976.

[15] N. Jones, Structural Impact, Cambridge: Cambridge University Press, 1997.

[16] K. W. Lee and L. C. Gan, Mathematical Modeling and Conceptual Design of a Shock Absorber for Lifting Equipment. Undergraduate Thesis. Monash University, Malaysia, 2005.

[17] Latch and Batchelor Ltd, Wire Rope for Every Application, Latch and Batchelor Ltd, viewed 24th August 2007, http://www.latchandbatchelor.co.uk/rope-info/rope-data/

[18] ANSYS Inc, Release 10 Documentation for ANSYS, Pennsylvania: ANSYS Inc.

[19] D. J. Ewins, Modal Testing: Theory, Practice and Application, 2nd Edition, Hertfordshire: Research Studies Press Ltd, 2000.